The Reasons Why Fractional Flow Reserve and Instance Wave-Free Ratio are Similar Using Wave Separation Analysis

Soohong Min
Jeju National University https://orcid.org/0000-0002-6201-2889
Gwansuk Kang
Stanford University School of Medicine
Dong-Guk Paeng
Jeju National University
Joon Hyouk Choi (valgom@hanmail.net)
Jeju National University School of Medicine, Jeju National University Hospital, Jeju, Korea
https://orcid.org/0000-0003-4245-1582

Research article

Keywords: Wave intensity analysis (WIA), fractional flow reserve (FFR), instantaneous wave-free ratio (IFR), coronary artery, wave separation analysis (WSA)

Posted Date: September 15th, 2020

DOI: https://doi.org/10.21203/rs.3.rs-70810/v1

Version of Record: A version of this preprint was published on January 25th, 2021. See the published version at https://doi.org/10.1186/s12872-021-01855-4.

The Reasons Why Fractional Flow Reserve and Instance Wave-Free Ratio are Similar using Wave Separation Analysis

Soohong Min[1, [a]], Gwansuk Kang[2, [b]], Dong-Guk Paeng[1, [c]*], Joon Hyouk Choi[3, [d]*]

[1] Department of Ocean System Engineering, Jeju National University, Jeju, Korea

[2] Division of Gastroenterology and Hepatology, Stanford University School of Medicine, Stanford, CA, USA

[3] Department of Cardiology, Jeju National University School of Medicine, Jeju National University Hospital, Jeju, Korea

*Corresponding author: Joon Hyouk Choi

[a] **tnghd337@naver.com**

[b] **gwansuk@stanford.edu**

[c] **paeng@jejunu.ac.kr**

[d]* **valgom@hanmail.net**

Abstract

Background and Objectives: Fractional flow reserve (FFR) and instantaneous wave-free ratio (iFR) are the two most commonly used coronary indices of physiological stenosis severity based on pressure. To minimize the effect of wedge pressure (P_{wedge}), FFR is measured during hyperemia conditions, and iFR is calculated as the ratio of distal and aortic pressures (P_d/P_a) in the wave-free period. The goal of this study was to predict P_{wedge} using the backward wave (P_{back}) through wave separation analysis (WSA) and to reflect the effect of P_{wedge} on FFR and iFR to identify the relationship between the two indices.

Methods: An *in vitro* circulation system was constructed to calculate P_{wedge}. The measurements were performed in cases with stenosis percentages of 48, 71, and 88% and with hydrostatic pressures of 10 and 30 mmHg. Then, the correlation between P_{back} by WSA and P_{wedge} was calculated. *In vivo* coronary flow

and pressure were simultaneously measured for 11 vessels in all patients. The FFR and iFR values were reconstructed as the ratios of forward wave at distal and proximal sites during hyperemia and at rest, respectively.

Results: Based on the *in vitro results*, the correlation between P_{back} and P_{wedge} was high (r=0.990, p<0.0001). *In vivo* results showed high correlations between FFR and reconstructed FFR (r=0.992, p<0.001) and between iFR and reconstructed iFR (r=0.930, p<0.001).

Conclusions: Reconstructed FFR and iFR were in good agreement with conventional FFR and iFR. FFR and iFR can be expressed as the variation of trans-stenotic forward pressure, indicating that the two values are inferred from the same formula under different conditions.

Keywords

Wave intensity analysis (WIA), fractional flow reserve (FFR), instantaneous wave-free ratio (IFR), coronary artery, wave separation analysis (WSA)

Background

Fractional flow reserve (FFR) is considered the "gold standard" among aggressive physiological diagnostic methods for determining the percutaneous coronary intervention of intermediate lesions in patients with stable angina[1]. Therefore, FFR was used as a comparative group for instantaneous wave-free ratio (iFR) in some studies. In these studies, iFR has been reported to be faster, less uncomfortable, and not inferior compared to FFR[2, 3].

To explain FFR theoretically, coronary wedge pressure (P_{wedge}) is a very important factor. FFR is measured when P_{wedge} is minimized by pharmacological hyperemia[4]. The P_{wedge} wave is characterized by rapid decline in and formation of baseline in pre-systole[5]. This event is explained by backward-propagating suction-waves in wave intensity analysis (WIA) and loss of the Windkessel effect due to occlusion[6, 7]. The Windkessel effect is defined as the condition where the pressure does not fall to zero

47 due to capacitive elements and resistance[8]. If iFR can also be explained by P_{wedge} or backward wave
48 through wave separation analysis (WSA), we can explain how the two indices are similar or different.
49 Thus, iFR could be measured when P_{wedge} is minimized during the wave-free period of diastole without
50 hyperemia.
51 This study was based on the assumption that coronary pressure waves can be separated into constituent
52 forward (P_{for}) and backward (P_{back}) waves using WSA. We attempted to prove this assumption as
53 follows: (1) P_{back} can replace P_{wedge} from an *in vitro* experimental study; and (2) FFR and iFR can be
54 reconstructed using P_{back} obtained from WSA and compared with conventional FFR and iFR from *in vivo*
55 measurement results. This study may be the first to identify similarities and differences between FFR and
56 iFR using WSA.

57 **Experiment and Method**

58 **Theoretical background**

59 The iFR is defined as the ratio of distal pressure (P_d) to aortic pressure (P_a) at rest during a wave-free
60 period, as shown in Equation 1:

61 $$\mathbf{iFR} = \frac{\mathbf{P_d}}{\mathbf{P_a}} \boldsymbol{at\ rest\ during\ wave-free\ period}\ [\mathbf{1}]$$

62 Assuming that P_{wedge} or $P_{back} + P_{static}$ is baseline in the wave-free period, the slopes of P_d and $P_{a,}$ and for
63 $P_{for}(prox)$ and $P_{for}(dist)$ in pre-systolic phase could be the same, as shown in Figure 1. Thus,
64 reconstructed iFR is redefined as follows in Equation 2:

65 $$\mathbf{reconstructed\ iFR} = \frac{\mathbf{P_d} - (\mathbf{P_{back}} + \mathbf{P_{static}})}{\mathbf{P_a} - (\mathbf{P_{back}} + \mathbf{P_{static}})} \approx \frac{\mathbf{P_{for}}(\boldsymbol{dist})}{\mathbf{P_{for}}(\boldsymbol{prox})}\ (\boldsymbol{at\ resting})\ [\mathbf{2}]$$

66 Reconstructed iFR is calculated as the average pressure of an entire cycle at rest and is not the same as
67 conventional iFR, which is determined only in the wave-free period. Reconstructed iFR, which is the ratio
68 of P_{for} at distal and proximal locations averaged over a whole cycle, is assumed to be similar to

conventional iFR. This assumption will be shown to be appropriate by in vitro and in vivo experimental results in this study.

$$\mathbf{FFR} = \frac{\mathbf{P}_d - \mathbf{P}_{wedge}}{\mathbf{P}_a - \mathbf{P}_{wedge}} \ (\boldsymbol{at\ hyperemia}) \ \mathbf{[3]}$$

FFR is defined as the ratio of distal pressure ($\mathbf{P}_d$) and aortic pressure ($\mathbf{P}_a$) when the effect of $\mathbf{P}_{wedge}$ is subtracted using hyperemia as shown in Equation 3:

$$\mathbf{reconstructed\ FFR} = \frac{\mathbf{P}_d - (\mathbf{P}_{back} + \mathbf{P}_{static})}{\mathbf{P}_a - (\mathbf{P}_{back} + \mathbf{P}_{static})} = \frac{\mathbf{P}_{for}(\boldsymbol{dist})}{\mathbf{P}_{for}(\boldsymbol{prox})} \ (\boldsymbol{at\ hyperemia}) \ [\mathbf{4}]$$

Reconstructed FFR is the ratio of $\mathbf{P}_{for}$ at the distal and proximal locations when $\mathbf{P}_{wedge}$ is assumed to be $\mathbf{P}_{back} + \mathbf{P}_{static}$.

WIA was performed to obtain wave-free periods using representative flow speed (U) and pressure (P) as in Equations 5 and 6:

$$\mathbf{WI}(+) = \frac{\mathbf{1}}{\mathbf{4}\boldsymbol{\rho c}}\left(\frac{\boldsymbol{dP}}{\boldsymbol{dt}} + \boldsymbol{\rho c}\frac{\boldsymbol{dU}}{\boldsymbol{dt}}\right)^{\mathbf{2}} \ [\mathbf{5}]$$

$$\mathbf{WI}(-) = \frac{\mathbf{1}}{\mathbf{4}\boldsymbol{\rho c}}\left(\frac{\boldsymbol{dP}}{\boldsymbol{dt}} - \boldsymbol{\rho c}\frac{\boldsymbol{dU}}{\boldsymbol{dt}}\right)^{\mathbf{2}} \ [\mathbf{6}]$$

where ϱ is the density of blood (1050 kg^{-3}), and c is wave speed calculated using the single-point equation. The wave-free period is defined as the time from WI (-) = 0 to the end of diastole for 5 ms[7].

WSA was performed to obtain P_{for} and P_{back} using representative flow (F(t)) and pressure (P(t)) obtained from Equations 7 and 8:

$$\mathbf{P}_{for}(\mathbf{t}) = \frac{[\boldsymbol{P(t)} + \mathbf{Z}_c \times \boldsymbol{F(t)}]}{\mathbf{2}} \ [\mathbf{7}]$$

$$\mathbf{P}_{back}(\mathbf{t}) = \frac{[\boldsymbol{P(t)} - \mathbf{Z}_c \times \boldsymbol{F(t)}]}{\mathbf{2}} \ [\mathbf{8}]$$

where Z_c is characteristic impedance and is defined as an input impedance (Z_i) in the absence of wave reflection. Z_i is defined as resistance or impedance obtained by frequency analysis of representative pressure and blood flow using Fourier analysis[9]. At the same time, the modulus (division) and phase

(subtraction) of impedance were automatically calculated. Therefore, the impedance modulus at zero frequency (0-impedance) is mean pressure/mean flow. There are many methods of obtaining Z_c. In general, Z_c is defined as the modulus at the zero crossing point or a point close to zero in phase. The reason for this distinction is that the negative phase is the imaginary component of Fourier analysis. Previous studies have addressed Z_c with a fixed frequency[9-15]. However, Z_c can change depending on the situation[9]. In this study, we used flexible Z_c, which is defined as the average modulus of four harmonics of the fundamental frequency after zero crossing or close to zero in phase less than 10 Hz.

***In vitro* coronary artery circulation system**

In this study, we designed an *in vitro* coronary blood circulation system. As shown in Fig. 2, a catheter (Combo Wire XT ®, Volcano Corporation, San Diego, CA, USA) was inserted into a tube to simultaneously measure pressure and flow speed at the proximal and distal sites of stenosis. A pulsatile pump (Model 55-3305, Harvard Apparatus Corp., USA) was used to mimic heart motion. The pump rate was fixed to 60 rotations/min, and the operative phase ratio (OPR; systolic time over a cyclic time) was set to 60%. The tube was filled with 1.5 L of Doppler fluid (Model 707, ATS Laboratories, USA). The viscosity of this fluid (5 cP) is similar to that of human blood. The tube was an IXAK® silicon tube (SL-0710, TOMMYHECO, KOREA) with an internal diameter of 5 mm. To reflect stenotic coronary arteries in the system, stenotic vessels of 48, 71, and 88% (minimum vessel area/maximum vessel area) were created using a three-dimensional printer. The minimal luminal dimensions of each model were 28, 46, and 64%. A Windkessel model was constructed using an air tank to control blood flow, pressure waveforms, and phase differences, which were similar to those observed in the human coronary artery. This approach can eliminate negative pressure and exerts zero flow on the system. Measurements were performed at 20 mm proximal to the stenosis site, and a catheter was inserted 200 mm proximal to the site of stenosis.

We created three conditions. Fig. 2 (a) is the basal condition. There is a combination of forward and backward pressures in the coronary artery. Resistance with stenosis can be used to control the ratio of forward and backward flow. By adjusting the inner diameter of the resistor, the amount of fluid directed to the stenotic phantom can be adjusted. Therefore, the ratio of forward and backward flow can be controlled, which makes it possible to reproduce a human-like automatic control ability of the blood flow. If the inner diameter of the resistor is larger than that of each site of stenosis, a phenomenon occurs where the backward flow is larger than the forward flow. Forward and backward pressures were separated using WSA in this condition. The reservoir was used to control P_{static} in the blood flow system, which was adjusted by varying the height.

Fig. 2 (b) is a condition of forward flow only without backward flow. By adjusting the height of the reservoir, the P_{static} was controlled. High P_{static} and low P_{static} values are assumed to represent pre-hyperemia and hyperemia conditions, respectively. P_d/P_a values measured in pre-hyperemia and hyperemia conditions were assumed to indicate reconstructed iFR and reconstructed FFR, respectively. To confirm that this *in vitro* circulatory system mimics the blood flow of the coronary system, the flow speed of Case 2 (only forward condition) was divided by that of Case 1 (basal condition), and the ratio was compared to the coronary flow reserve.

Fig. 2 (c) depicts the P_{wedge}. In clinical practice, P_{wedge} is measured at a distal site when the artery is blocked with a balloon. To reflect this in the *in vitro* system, we blocked the branch point toward the coronary phantom through the valve. The measured pressure in this case was compared with the backward pressure that was calculated using WSA.

***In vivo* experiment**

The study protocol was approved by the institutional review board of Jeju National University Hospital (2016-07-011).

Coronary angiography and pressure-flow measurements were obtained using standard techniques[16]. Angiographic views were obtained following administration of intracoronary nitrate in all cases (200 or 300 μg). We used 0.014-inch pressure and Doppler sensor-tipped wires (ComboWire XT, Volcano Corporation, San Diego, CA, USA). The distal pressure was removed and equalized to the aortic pressure at the coronary ostium before being positioned at least three vessel diameters distal to the site of stenosis. Adenosine was administered for hyperemia by intravenous infusion based on 11 measurements (140 μg/kg/min). When a ComboWire was used, the electrocardiogram, pressures, and flow velocity signals were directly extracted from the digital archive of the device console (ComboMap, Volcano Corporation). Data were analyzed off-line, using a custom software package designed by Labview (National Instruments, Austin, TX, USA). Stenosed vessels were defined as vessels that had an angiographically visible stenosis from 40–70% severity, as determined visually by an operating physician at the time of coronary angiography.

Resting indices were calculated at a time of stability, allowing for a return to stable baseline conditions after any preceding injection of contrast or saline. Hyperemic indices were determined during stable hyperemia, excluding cases with ectopy or conduction delay. Representative flow and pressure waves were obtained by an average method using recordings of 5–15 consecutive cycles both at rest and during hyperemia. These procedures were necessary to achieve linearity and time invariance. FFR and iFR were calculated as the ratio of mean P_d to P_a at hyperemia during a whole cycle and at rest during a wave-free period, respectively.

Statistical analysis

All statistical analyses were performed using the Statistical Package for the Social Sciences (SPSS), version 23.0 software (SPSS Statistics for Macintosh, IBM Corp. Armonk, NY, USA). The values of continuous variables are mean and standard deviation (SD), and categorical variables are expressed as frequency and

158 percentage. The comparison of continuous variables between groups was performed using the
159 independent sample t-test, and the categorical variables were assessed with a chi-square test. The
160 correlation analysis between groups was performed by simple correlation analysis. For each statistic, the
161 significance level was less than 0.05.

162 **Result**

163 ***In vitro* experiment**

164 A total of 18 cases were analyzed according to stenoses (48, 71, and 88%), and P_{static} (10 and 30 mmHg)
165 values obtained from mock circulatory experiments. The measured and calculated data are summarized
166 in Table 1.

167 **Table 1.** Measured pressure and distal flow speed in the 3 models of stenosis.

Stenosis	P_{static}	Case 1 Basal condition					Case 2 Forward flow condition			Case3 Wedge condition
(%)	(mmHg)	Observed Indices			Calculated Indices		Observed Indices			
		P_a (mmHg)	P_d (mmHg)	Distal Flow (cm/s)	P_{for} (mmHg)	P_{back} (mmHg)	P_a (mmHg)	P_d (mmHg)	Distal flow (cm/s)	P_{wedge} (mmHg)
48	10	20.2	18.2	13.98	10.9	7.3	23.27	18.83	29.9	19.7
48	30	40.6	40.4	16.40	27.8	12.6	44.50	40.29	31.9	40.1
71	10	21.7	19.3	23.53	11.3	7.0	25.30	16.14	37.7	15.0
71	30	43.1	41.2	24.76	29.3	12.0	46.64	41.26	37.7	40.1
88	10	36.6	18.5	29.46	11.8	6.7	44.62	20.51	35.4	19.3
88	30	57.0	38.4	30.92	29.0	9.5	64.05	38.45	37.4	38.4

168 P_a: coronary aortic pressure

169 P_{back}: backward pressure

170 P_d: coronary distal pressure

171 P_{for}: forward pressure

172 P_{static}: hydro static pressure

173 P_{wedge}: coronary wedge pressure

When the static pressure was 10 mmHg, the distal flow ratio (only forward flow/basal flow) according to stenosis increased to 2.2, 1.5, and 1.2 as the stenosis increased to 49, 71, and 88%, respectively. When the static pressure was 30 mmHg, the distal flow ratios were 2.5, 1.6, and 1.2 at stenosis rates of 49, 71, and 88%, respectively.

The P_d/P_a ratio for Case 1 decreased in the order of stenosis (48, 71, and 88%) at each P_{static} (10 mmHg, 0.81, 0.64, 0.46; 30 mmHg, 0.91, 0.88, 0.60, respectively). The distal flow ratio in high P_{static} was higher than that in low P_{static}.

The P_d/P_a ratio for Case 2 decreased in the order of stenosis (48, 71, and 88%) at each P_{static} (10 mm Hg, 0.90, 0.84, and 0.5; 30 mmHg, 1.00, 0.96, and 0.67, respectively). The change in P_d/P_a between Case 1 and Case 2 was larger for low P_{static} than for high P_{static}, as shown in Fig. 3.

The waveforms and magnitude of the observed P_{wedge} and $P_{back} + P_{static}$ were very similar (Figure 4). This trend was also observed in other cases. P_{wedge} always contains static pressure. Correlation with the $P_{back} + P_{static}$ and P_{wedge} was high (r = 0.990, p < 0.0001, Figure 5), and the slope was 1.0612.

***In vivo* experiment**

Nine patients in whom we were able to simultaneously measure blood flow and blood pressure in the proximal and distal regions were compared with pre- and post-hyperemia values of distal forward pressure P_{for} and \ distal backward pressure P_{back} using Z_c in 11 coronary blood vessels. The results are summarized in Table 2.

Table 2. Pressures (mmHg) at proximal and distal site at rest and hyperemia, and indices obtained from eleven coronary vessels in this study.

Patients	Vessels	FFR	iFR	P_a	P_d	P_{for} (distal)	P_{back} (distal)	P_{for} (distal)	P_{back} (distal)	Reconstructed FFR	Reconstructed iFR
				Resting		Resting		Hyperemia			
1	LAD	0.75	0.92	74.9	69.1	48.1	21	40.2	9.6	0.75	0.89
2	LAD	0.8	0.94	88.1	83.1	57.8	25.3	57.1	6.7	0.80	0.92

3	LAD	0.85	0.89	120.4	113.8	80.8	33	78.2	15.1	0.88	0.93
4	LAD	0.87	0.97	126.6	119.3	73.5	45.8	68.5	27.6	0.86	0.91
4	LCx	0.96	1.04	119.8	119.8	84.9	37.9	90	16.9	0.97	1.00
4	RCA	0.96	1.07	123.4	128.3	88.6	39.7	79.3	27.8	0.97	1.06
5	Ramus	0.94	0.99	102.5	101.3	60.2	40.1	70.3	20.5	0.95	0.98
6	LAD	0.73	0.82	109.7	96.0	70.3	25.7	68.6	11.6	0.70	0.84
7	LAD	0.8	0.98	108.8	104.5	62.4	42.1	59.2	28	0.81	0.94
8	LAD	0.66	0.74	88.1	67.6	39.6	28	45.2	12.2	0.66	0.66
9	LAD	0.89	1.07	105.7	108.3	63.7	44.6	75.1	15.2	0.90	0.94

FFR: fractional flow reserve

iFR: instantaneous wave-free ratio

$\mathbf{P_a}$: coronary aortic pressure

$\mathbf{P_d}$: coronary distal pressure

$\mathbf{P_{back}}$: backward pressure

$\mathbf{P_{for}}$: forward pressure

The correlations between conventional FFR and reconstructed FFR and between conventional iFR and reconstructed iFR were positive ($r = 0.992$, $p < 0.001$ and 0.930, $p < 0.001$, respectively; Fig. 6).

Discussion

In this study, coronary pressure waves could be separated into constituent forward (P_{for}) and backward (P_{back}) waves through WSA using frequency analysis. It could be said that P_{back} reflected P_{wedge} without P_{static} experimentally. It was shown that FFR and iFR could be expressed in trans-stenotic ΔP_{for} either with or without hyperemia, which indicated that the two indices were inferred by removing P_{wedge} or P_{back}. *In vivo,* FFR and iFR were reconstructed assuming that the P_{back} and P_{wedge}were very similar. The reconstructed indices were highly correlated with the conventional indices. Therefore, to our knowledge, this study is the first to identify similarities and differences between FFR and iFR using WSA.

Theoretical background of FFR and iFR through WSA

211 In this study, P_{back} was characterized as undergoing rapid decline and forming baseline observed during
212 pre-systole either with or without hyperemia. This finding is similar to the characteristics of P_{wedge} [5].
213 After forming the baseline of P_{back}, the slope of P_{for} was similar to the slope of coronary pressure. The
214 period of forming the baseline of P_{back} was similar to the wave-free period. Eventually, the amplitude of
215 P_{for} was smaller than the amplitude of coronary pressure (Figure 1). During the wave-free period, P_a, P_d,
216 and P_{for} could have the same slope because P_{back} forms the baseline. The ratio between the \ lines with
217 the same slope may be different, but the value in that interval is constant. iFR is defined as P_d/P_a in the
218 wave-free interval. Therefore, iFR may be related to P_{for}(distal) /P_{for}(proximal) during the wave-free
219 period. Furthermore, as the amplitude of P_{for} without P_{back} is low, the mean P_{for} of the whole cycle and
220 the mean P_{for} of the wave-free period may be similar as a factor of ratio. As a result, in this study,
221 reconstructed iFR was defined as P_{for}(distal) /P_{for}(proximal) in Equation 1. The reconstructed and
222 conventional iFRs showed a good correlation based on *in vivo* results.
223 During hyperemia, the theoretical FFR of the coronary artery (FFRcor) is $(P_d - P_w)/(P_a - P_w)$, while the
224 FFR of the myocardium (FFRmyo) is $(P_d - P_v)/(P_a - P_v)$, where P_v represents the mean central venous
225 pressure[4]. The FFR is the ratio between mean values. A mean value is decreased when both the peak
226 and the baseline are lowered. In this study, hyperemia mainly reduced the baseline of pressure (Figure 1).
227 Moreover, P_{back} was not zero but still decreased during hyperemia, and P_{for} was constant under the
228 Windkessel effect.
229 The difference between FFRcor and FFRmyo is described by collateral flow[4]. P_{wedge} is closely related to
230 the collateral flow[17]. In addition, hyperemia theoretically reflects the offset of P_{wedge} and P_v in the
231 conventional FFRs[4]. However, the values of the P_{wedge} or P_v would not be practically removed in
232 hyperemia.

The FFR is based on the assumption that resistances both with and without stenosis are the same. Without collateral flow, this assumption implies that FFRmyo progressively overestimates the FFR using flow with increasing stenosis severity[4]. Thus, an attempt has been made to overcome this mismatch in reconstructing the FFR using zero flow pressure (P_{zf}). The formula is as follows: FFR = $(P_d - P_{zf})/(P_a - P_{zf})$. FFR using P_{zf} was in good agreement with the FFR using flow compared to FFR using pressure[18]. Because of the diastolic characteristics of the coronary arteries, P_{zf} is independent of contraction and auto-regulation, showing conductance of the vessels and pure resistance[19-21]. However, P_{wedge} is generally smaller than P_{zf} due to the non-linearity of the pressure-flow relationship and existence of cardiac contraction either with or without collateral flow[21-23]. Conceptually, P_{back} by WSA was similar to P_{zf} in this study. This means that both FFR and iFR could be trans-stenotic ΔP_{for}, which can be expressed using the same formula, although their methods are different (Equations 1 and 2).

Difference between FFR and iFR

In order to replace the FFR using flow with FFR using pressure, hyperemia is required to offset P_{wedge} and P_v[4]. As mentioned above, the reconstructed iFR was calculated by subtracting P_{back} at rest, which is assumed to be P_{wedge}. Theoretically, P_{for} can be determined by the stroke volume, which is related with inflow, resistance, compliance, and volume capacity, because the Windkessel effect is observed and systolic resistance by subtracting P_{for} is absent[8]. It is similar to systemic circulation. When administered for hyperemia, adenosine is reported to have little effect on the stroke volume or ejection fraction[24]. There is no significant change in blood volume without bleeding. Therefore, the difference in P_{for} with or without hyperemia is mainly dependent on resistance. The change of resistance according to the situation from rest to hyperemia could be the change of P_{static} or P_v. Thus, the difference between iFR and FFR is likely to be the difference of P_{for} in relation to P_{static} or P_v rather than P_{wedge} or P_{back}.

As myocardium oxygen consumption (MVO_2) increases due to enlargement of micro-vessels, resistance is reduced, and flow is increased. This trend is mainly regulated by the adenosine and nitric oxide (NO) metabolites in the myocardium. In the presence of significant stenosis, the role of adenosine may be activated in micro-vessels, so the reactivity of hyperemia by adenosine may be lowered. In other words, resistance due to pharmacological hyperemia may be smaller in significant stenosis than in nonsignificant stenosis[25, 26].

The incidence of clinically appropriate hyperemia is not well known. In fact, it is difficult to verify hyperemia even with constant drug increases or drug changes. Thus, nonsignificant changes of P_{for} during hyperemia may be explained by the limitations of the assumption of constant resistance either with or without stenosis in FFR and pharmacological hyperemia with inappropriate offsets of P_{wedge} and P_v.

Nevertheless, this study assumes that P_{for} is the primary factor for determining iFR and FFR using pressure. This assumption was confirmed by *in vivo* and *in vitro* results.

Limitation

In this paper, we tried to reflect the characteristics of various coronary arteries such as blood flow and pressure waveforms, in the human body. There are many differences in blood flow and pressure waveforms in human coronary arteries. However, this variation did not pose a problem because we used the average values for pressure and blood flow.

It cannot be said that P_{back} reflects P_{wedge} experimentally. The constituent waves from WSA are the estimated values[10]. Moreover, the purpose of this study was to prove that iFR and FFR share the same formula. Therefore, the most important factors are morphological pattern and phase; acquiring accurate values was not the main goal. Accordingly, several trials of WSA were performed that considered many Z_c values. The results from various trials of WSA showed a similar pattern.

According to Van Huis et al., Z_c increased during hyperemia[14]. However, Z_c decreased in this study. Although this result cannot be explained, it is inferred that there are differences in the species or drugs used for hyperemia. To verify this hypothesis, additional experiments for Z_c will be needed.

Conclusions

In this study, we calculated P_{back} in the coronary artery using WSA and confirmed that the correlation between P_{back} and P_{wedge} was high. The FFR and iFR were reconstructed by reflecting P_{wedge} calculated through P_{back}. It could be proved deductively that FFR and iFR can be expressed in the trans-stenotic ΔP_{for}. Therefore, the two indices are inferred from the same formula under different conditions. Similarities and differences between iFR and FFR were thus confirmed.

Abbreviations

FFR: Fractional flow reserve; iFR: wave-free ratio; P_{wedge}: wedge pressure; WSA: wave separation analysis; WIA: wave intensity analysis; P_{for}: forward pressure; P_{back}: backward pressure; P_d: distal pressure; P_a: aortic pressure; P_{static}: static pressure;

Declarations

Ethics approval and consent to participate

Written consent was obtained from all participants, and the study protocol was approved by the institutional review board of Jeju National University Hospital (2016-07-011).

Consent for publication

Not applicable

Availability of data and materials

The datasets used and/or analyzed during the current study are available from the corresponding author on reasonable request.

Competing interests

The authors declare no conflict of interest.

Funding

This work was supported by the National Research Foundation of Korea(NRF) grant funded by the Korea government (MSIT, No. 2018R1A2B2007997) and the research grant from Jeju national university hospital development fund in 2016.

Authors' contributions

SM performed validation experiment, analyzed the data, and was a major contributor in writing the manuscript. GK developed the software that calculates various pressure. DP gave feedback on the progress of all experiments and helped to draft the manuscript. JC designed and coordinated the study, conducted all clinical trials and helped to draft the manuscript. All authors read and approved the final manuscript.

Acknowledgments

Not applicable

References

1. Fihn SD, Blankenship JC, Alexander KP, Bittl JA, Byrne JG, Fletcher BJ, et al. 2014 ACC/AHA/AATS/PCNA/SCAI/STS focused update of the guideline for the diagnosis and management of patients with stable ischemic heart disease: A report of the American College of Cardiology/American Heart Association Task Force on Practice Guidelines, and the American Association for Thoracic Surgery, Preventive Cardiovascular Nurses Association, Society for Cardiovascular Angiography and Interventions, and Society of Thoracic Surgeons. J Am Coll Cardiol. 2014;64(18):1929-49.

2. Götberg M, Christiansen EH, Gudmundsdottir IJ, Sandhall L, Danielewicz M, Jakobsen L, et al. Instantaneous wave-free ratio versus fractional flow reserve to guide PCI. N Engl J Med. 2017;376(19):1813-23.

3. Davies JE, Sen S, Dehbi H, Al-Lamee R, Petraco R, Nijjer SS, et al. Use of the instantaneous wave-free ratio or fractional flow reserve in PCI. N Engl J Med. 2017;376(19):1824-34.

4. Pijls NH, van Son JA, Kirkeeide RL, De Bruyne B, Gould KL. Experimental basis of determining maximum coronary, myocardial, and collateral blood flow by pressure measurements for assessing functional stenosis severity before and after percutaneous transluminal coronary angioplasty. Circulation 1993;87(4):1354-67.

5. Pacold I, Hwang MH, Piao ZE, Scanlon PJ, Loeb HS. The mechanism and significance of ventricularization of intracoronary pressure during coronary angiography. Am Heart J. 1989;118(6):1161-6.

6. Westerhof N, Segers P, Westerhof BE. Wave separation, wave intensity, the reservoir-wave concept, and the instantaneous wave-free ratio: Presumptions and principles. Hypertension 2015;66(1):93-8.

7. Davies J, Whinnett Z, Francis D, Manisty C. Guado-Sierra J, Willson K, et al. evidence of a dominant backward-propagating “suction” wave responsible for diastolic coronary filling in humans, attenuated in left ventricular hypertrophy. Circulation 2006;113:1768-78.

8. Westerhof N, Lankhaar J, Westerhof BE. The arterial Windkessel. Med Biol Eng Comput. 2009;47(2):131-41.

9. O'Rourke MF, Taylor MG. Input impedance of the systemic circulation. Circ Res. 1967;20(4):365-80.

10. O'Rourke MF, Hartley C, McDonald DA. McDonald's blood flow in arteries: Theoretic, experimental, and clinical principles. Arnold; 1998.

11. Bergel DH, Milnor WR. Pulmonary vascular impedance in the dog. Circ Res. 1965;16(5):401-15.

12. Milnor WR, Bertram CD. The relation between arterial viscoelasticity and wave propagation in the canine femoral artery in vivo. Circ Res. 1978;43(6):870-9.

13. Stergiopulos N, Westerhof BE, Westerhof N. Total arterial inertance as the fourth element of the Windkessel model. Am J Physiol Heart Circ Physiol. 1999;276(1):H81-8.

14. Van Huis GA, Sipkema P, Westerhof N. Coronary input impedance during cardiac cycle as determined by impulse response method. Am J Physiol. 1987;253(2 Pt 2):H317-24.

15. Cox RH, Bagshaw RJ. Baroreceptor reflex control of arterial hemodynamics in the dog. Circ Res. 1975;37(6):772-86.

16. Kern MJ, Lerman A, Bech J, De Bruyne B, Eeckhout E, Fearon WF, et al. Physiological assessment of coronary artery disease in the cardiac catheterization laboratory: A scientific statement from the American Heart Association Committee on Diagnostic and Interventional Cardiac Catheterization, Council on Clinical Cardiology. Circulation 2006;114(12):1321-41.

17. Mohri M, Egashira K, Kuga T, Shimokawa H, Takeshita A. Correlations between recruitable coronary collateral flow velocities, distal occlusion pressure, and electrocardiographic changes in patients undergoing angioplasty. Jpn Circ J. 1997;61(12):971-8.

18. Claessens TE, Van Herck PL, Matthys KS, Segers P, Vrints CJ, Verdonck PR. Influence of zero flow pressure on fractional flow reserve. Biomech Model Mechanobiol. 2004;3(1):48-55.

19. Bellamy RF. Diastolic coronary artery pressure-flow relations in the dog. Circ Res. 1978;43(1):92-101.

20. Mancini GB, McGillem MJ, DeBoe SF, Gallagher KP. The diastolic hyperemic flow versus pressure relation. A new index of coronary stenosis severity and flow reserve. Circulation 1989;80(4):941-50.

21. Spaan JA, Piek JJ, Hoffman JI, Siebes M. Physiological basis of clinically used coronary hemodynamic indices. Circulation 2006;113(3):446-55.

366 22. Messina LM, Hanley FL, Uhlig PN, Baer RW, Grattan MT, Hoffman JI. Effects of pressure gradients
367 between branches of the left coronary artery on the pressure axis intercept and the shape of steady state
368 circumflex pressure-flow relations in dogs. Circ Res. 1985;56(1):11-9.
369 23. Downey JM, Kirk ES. Inhibition of coronary blood flow by a vascular waterfall mechanism. Circ Res.
370 1975;36(6):753-60.
371 24. Ogilby JD, Iskandrian AS, Untereker WJ, Heo J, Nguyen TN, Mercuro J. Effect of intravenous
372 adenosine infusion on myocardial perfusion and function. hemodynamic/angiographic and scintigraphic
373 study. Circulation 1992;86(3):887-95.
374 25. Gould KL, Lipscomb K, Hamilton GW. Physiologic basis for assessing critical coronary stenosis:
375 Instantaneous flow response and regional distribution during coronary hyperemia as measures of
376 coronary flow reserve. Am J Cardiol. 1974;33(1):87-94.
377 26. Gould KL, Kirkeeide RL, Buchi M. Coronary flow reserve as a physiologic measure of stenosis
378 severity. J Am Coll Cardiol. 1990;15(2):459-74.

379

380 **Figures**

381 **Figure 1 Changes in pressures before and after Hyperemia and wave free period extraction**
382 **through WIA analysis.** a) Aortic and distal pressures (P_a, P_d), forward and backward waves
383 (P_{for}, P_{back}) in a cycle at pre-hyperemia and hyperemia, and horizontal lines are their average
384 values over a cycle. P_a decreased little but P_d decreased more at hyperemia. Although overall
385 P_{back} decreases a lot at hyperemia, there is little change in P_{for} between pre-hyperemia and
386 hyperemia (b) Wave free period was extracted through wave intensity analysis (WIA) as shown
387 in green boxes.

Figure 2 An *in vitro* coronary circulation system. Three conditions were created as (a), (b) and (c). (a) Basal condition, in which both forward and backward flows existed. Resister was used to control the ratio of forward and backward flow, and the pressure and blood flow were stabilized using the Windkessel model. (b) Only forward condition, in which backward flow was blocked. By adjusting the height of the reservoir, the P_{static} was controlled. High P_{static} is assumed to be pre-hyperemia and low P_{static} is assumed to be hyperemia. (c) Only backward flow condition, in which forward flow was blocked for measuring.

Figure 3 P_d/P_a in Case1 and 2 at 3 stenosis when P_{static} was 30 and 10 mmHg. When the static pressure was 30 mmHg(High hydrostatic pressure), P_d/P_a in case 2 was set as reconstructed iFR, and when the static pressure was 10 mmHg(Low hydrostatic pressure), P_d/P_a in case 2 was set as reconstructed FFR.

Figure 4 The waveform of P_{wedge} and P_{back}. The static pressure was (a) 10 and (b) 30 mmHg at stenosis 48%. Each static pressure was added to P_{back}.

Figure 5 The correlation between observed wedge pressure(P_{wedge}) and calculated wedge pressure($P_{back} + P_{static}$). The correlation was high (r = 0.990, p<0.0001) and slope was 1.0612.

Figure 6 Correlation between (a) FFR and reconstructed FFR, (b) iFR and reconstructed iFR. Both graphs show a high correlation.

Figures

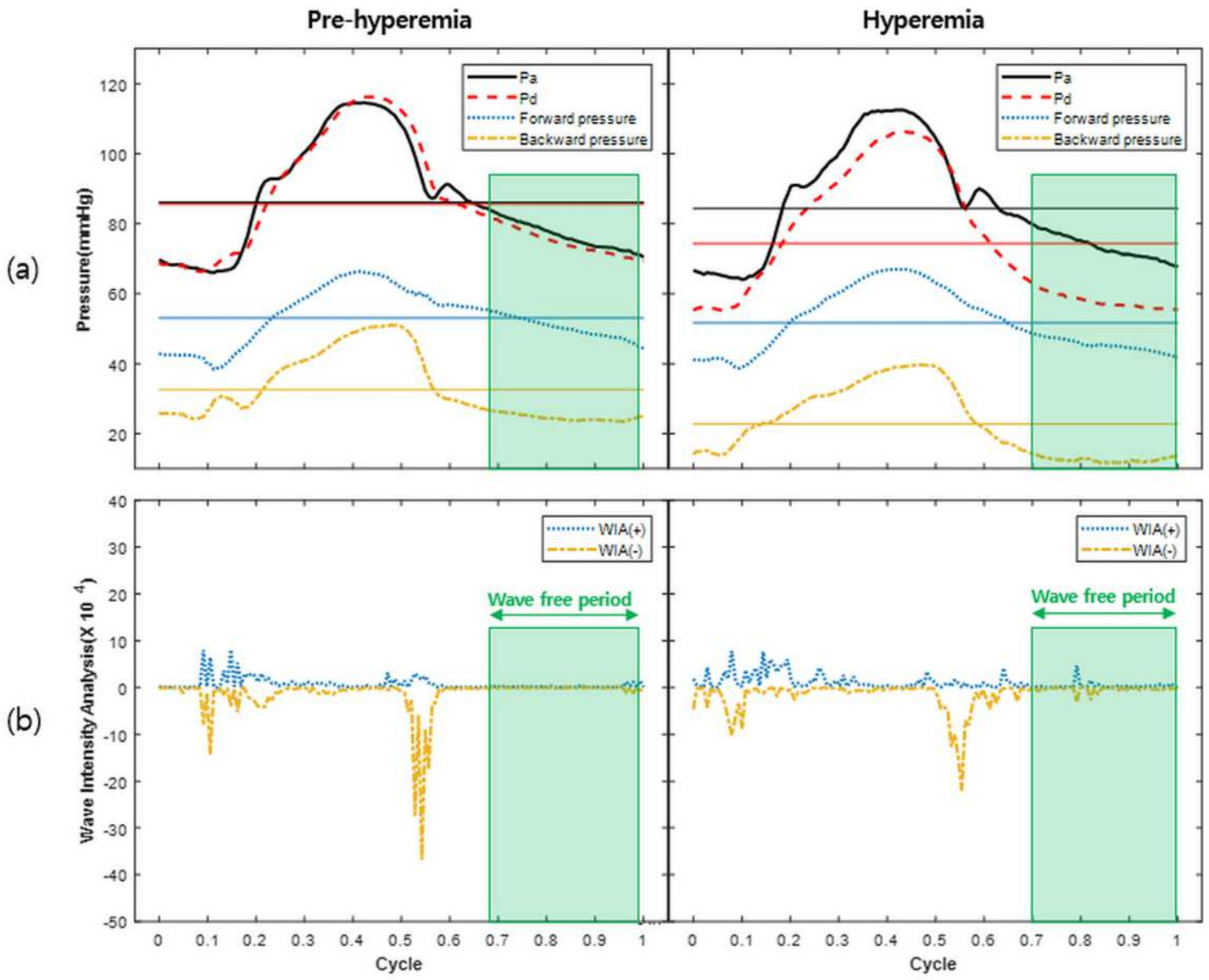

Figure 1

Changes in pressures before and after Hyperemia and wave free period extraction through WIA analysis. a) Aortic and distal pressures (P_a, P_d), forward and backward waves (P_for, P_back) in a cycle at pre-hyperemia and hyperemia, and horizontal lines are their average values over a cycle. P_a decreased little but P_d decreased more at hyperemia. Although overall P_back decreases a lot at hyperemia, there is little change in P_for between pre-hyperemia and hyperemia (b) Wave free period was extracted through wave intensity analysis (WIA) as shown in green boxes.

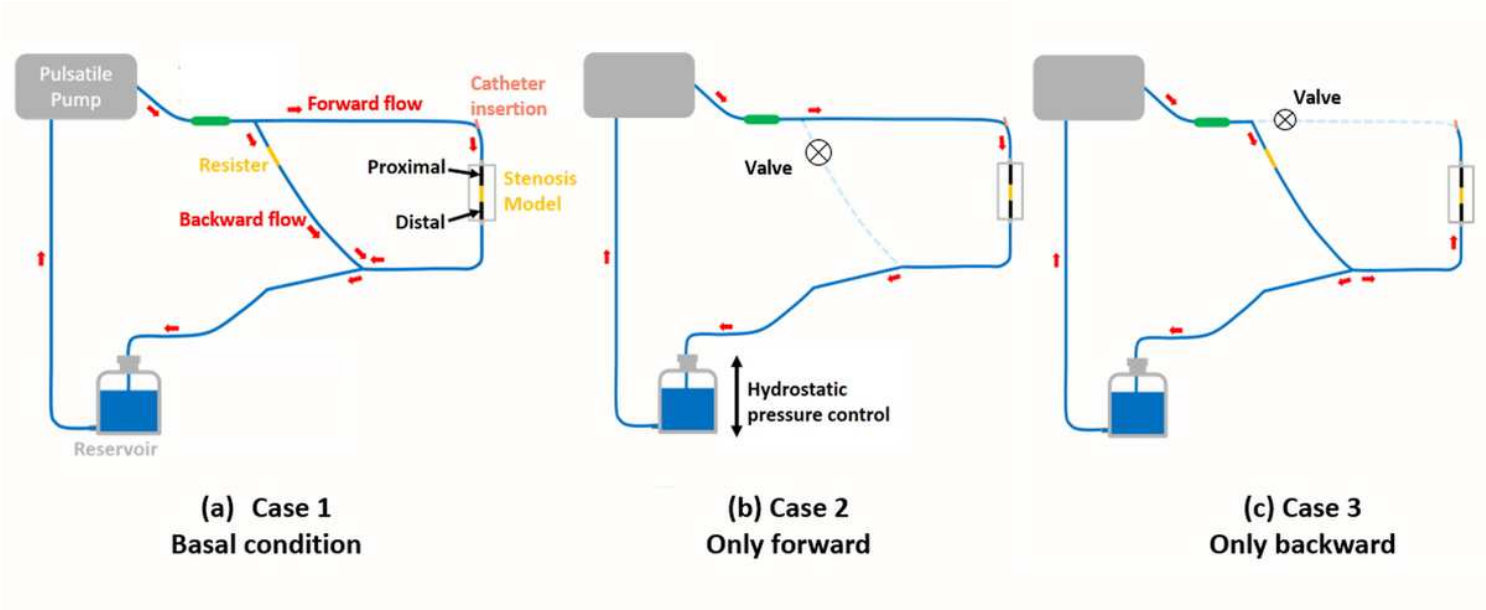

Figure 2

An in vitro coronary circulation system. Three conditions were created as (a), (b) and (c). (a) Basal condition, in which both forward and backward flows existed. Resister was used to control the ratio of forward and backward flow, and the pressure and blood flow were stabilized using the Windkessel model. (b) Only forward condition, in which backward flow was blocked. By adjusting the height of the reservoir, the P_static was controlled. High P_static is assumed to be pre-hyperemia and low P_static is assumed to be hyperemia. (c) Only backward flow condition, in which forward flow was blocked for measuring.

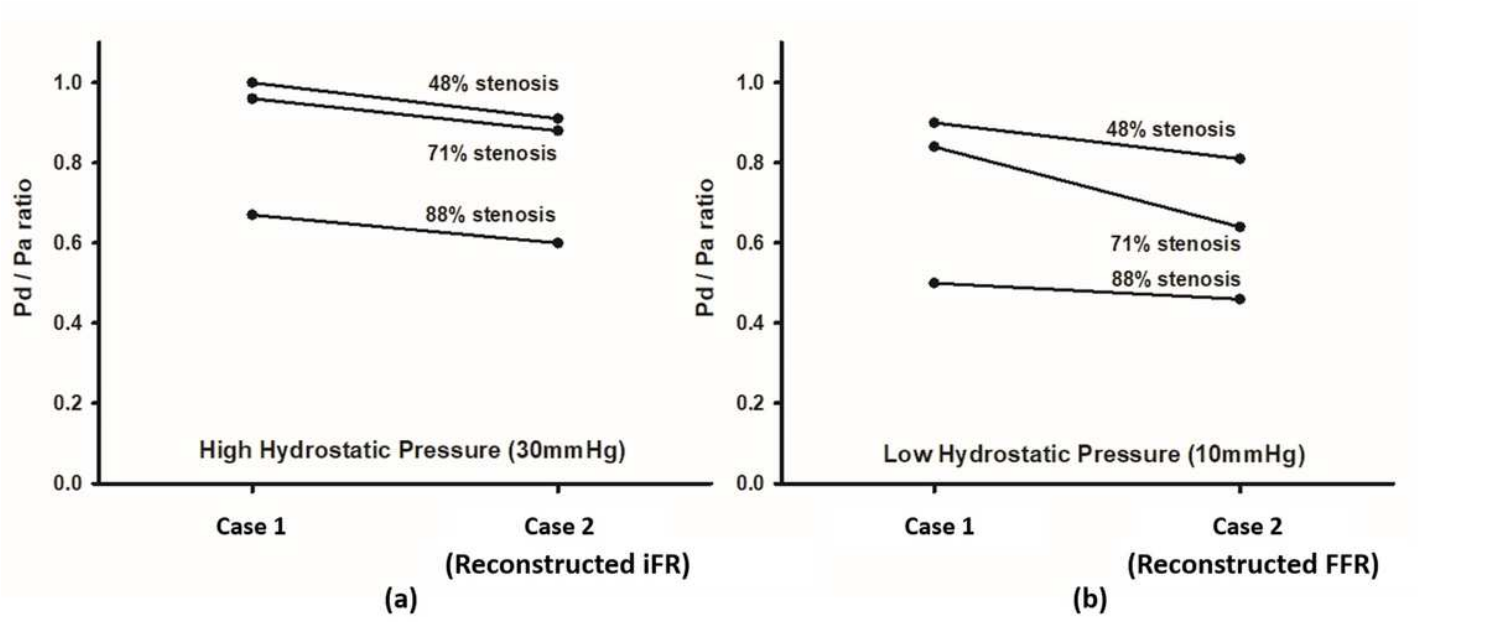

Figure 3

P_d/P_a in Case1 and 2 at 3 stenosis when P_static was 30 and 10 mmHg. When the static pressure was 30 mmHg(High hydrostatic pressure), P_d/P_a in case 2 was set as reconstructed iFR, and when the

static pressure was 10 mmHg(Low hydrostatic pressure), P_d/P_a in case 2 was set as reconstructed FFR.

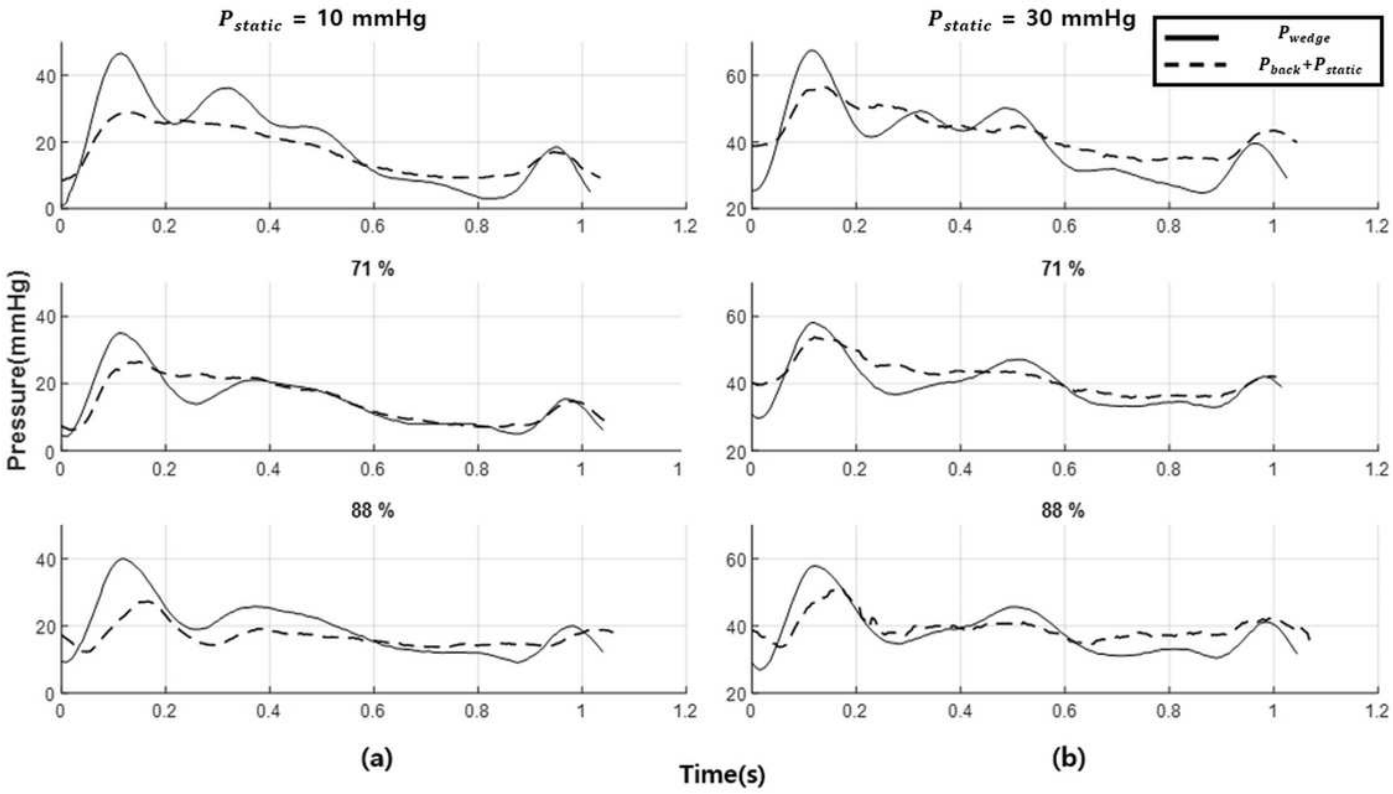

Figure 4

The waveform of P_wedge and P_back. The static pressure was (a) 10 and (b) 30 mmHg at stenosis 48%. Each static pressure was added to P_back.

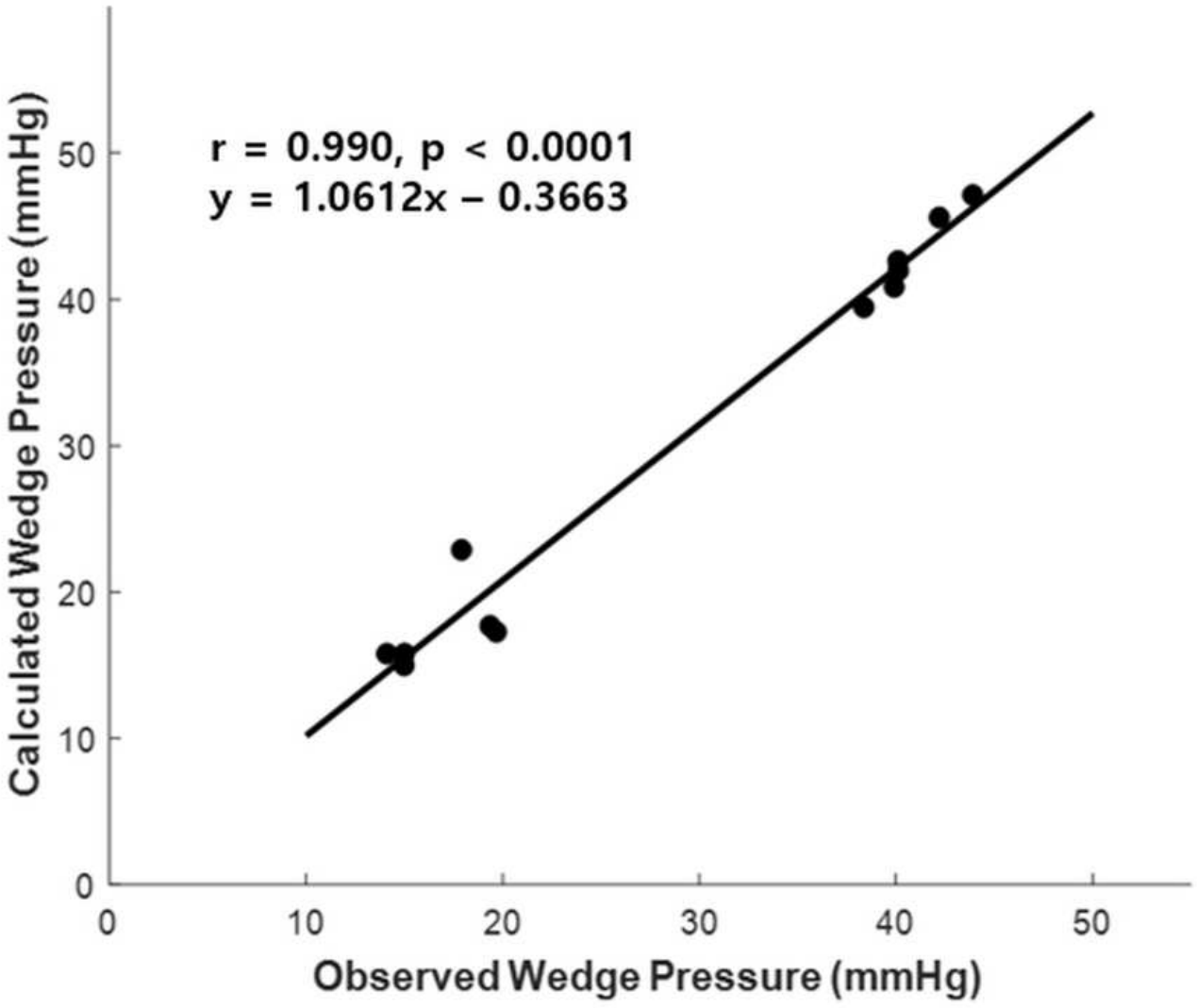

Figure 5

The correlation between observed wedge pressure(P_wedge) and calculated wedge pressure(P_back+P_static). The correlation was high (r = 0.990, p<0.0001) and slope was 1.0612.

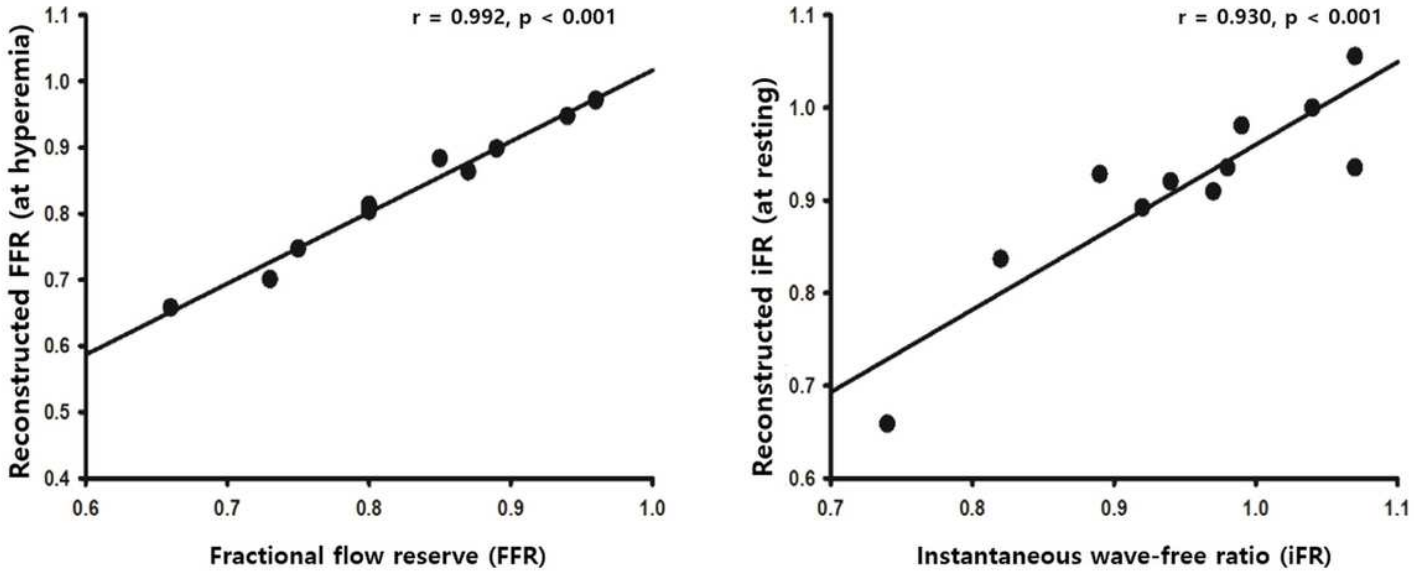

Figure 6

Correlation between (a) FFR and reconstructed FFR, (b) iFR and reconstructed iFR. Both graphs show a high correlation.